

# Reaction Densification of $\alpha'$ -SiAlON: II, Densification Behavior

Mohan Menon and I-Wei Chen\*

Department of Materials Science and Engineering, University of Michigan, Ann Arbor, Michigan 48109-2136

Reaction hot-pressing behavior of  $\alpha$ - $\text{Si}_3\text{N}_4$ ,  $\text{Al}_2\text{O}_3$ , AlN, and  $\text{M}_2\text{O}_2$  powder mixtures ( $M = \text{Li, Mg, Ca, Y, Nd, Sm, Gd, Dy, Er, and Yb}$ ) forming  $\alpha'$ -SiAlON has been studied. Five characteristic temperatures are found to control the densification behavior of these materials. The densification proceeded in three major stages. The first two stages were formation of ternary oxide eutectic and wetting of majority nitride powder. The third stage involved dissolution/melting of intermediate phase. Variation from this behavior sometimes occurs due to localization of wetting liquid at AlN, extremely high melting/dissolution temperature of  $\text{Mg}_2\text{Al}_4\text{Si}_2\text{O}_{18}$  and Nd and Sm melilite, and secondary precipitation of Dy- $\alpha'$ -SiAlON. The dominant densification mechanism was found to be massive particle rearrangement, irrespective of the wetting and dissolution/melting behavior. The efficiency of this mechanism is mostly affected by the amount of available liquid and less by its viscosity. Fully dense, single-phase ceramics were obtained in all cases except Mg when hot-pressed at a constant heating rate to 1750°C, and considerably lower temperatures for Li, Ca, Gd, Dy, Er, and Yb-SiAlON when held isothermally.

## I. Introduction

SINCE the concept of "transient liquid sintering" was introduced, intensive investigations have been done on the reaction sintering of SiAlON in the metal oxide- $\text{Si}_3\text{N}_4$ -AlN-SiO<sub>2</sub>-Al<sub>2</sub>O<sub>3</sub> system.<sup>1-12</sup> Some of the earliest work was carried out in the MgO- $\text{Si}_3\text{N}_4$ -AlN-SiO<sub>2</sub> system by Lewis *et al.*<sup>1-3</sup> They found that a transient phase which formed during the hot-pressing of  $\alpha$ - $\text{Si}_3\text{N}_4$  with MgO reacted with  $\alpha$ - $\text{Si}_3\text{N}_4$  above 1400°C to form  $\beta$ - $\text{Si}_3\text{N}_4$  and a vitreous phase.<sup>1</sup> This reaction was found to expedite the sintering kinetics. Further, they found that the sintering kinetics and the reaction pathway of a mixture of MgO- $\text{Si}_3\text{N}_4$ -AlN-SiO<sub>2</sub> depended on the amount of MgO.<sup>2,3</sup> The addition of Y<sub>2</sub>O<sub>3</sub>, instead of MgO to a  $\text{Si}_3\text{N}_4$ -AlN-SiO<sub>2</sub> mixture resulted in a sample with diphasic  $\beta'$  SiAlON-Y<sub>3</sub>Al<sub>5</sub>O<sub>12</sub> (YAG) microstructure with improved mechanical properties.<sup>4</sup> Boskovic *et al.* used the concept of transient liquid sintering to obtain dense  $\beta'$ -SiAlON ceramics in the  $\text{Si}_3\text{N}_4$ -AlN-SiO<sub>2</sub>-Al<sub>2</sub>O<sub>3</sub> plane.<sup>5-7</sup> In their study, they too found that the sintering kinetics depended on the composition of starting powder mixtures, even though the final composition was the same. In these and other reaction hot-pressing studies, the densification mechanisms were identified to be either solution-reprecipitation,<sup>1-4</sup> fast particle rearrangement,<sup>10</sup> Coble creep,<sup>10</sup> or grain boundary sliding.<sup>9,11</sup>

Recently, Hwang and Chen found that reaction hot pressing of  $\alpha'$ - and  $\alpha'$ - +  $\beta'$ -Y-SiAlON took place in three stages.<sup>12</sup> Further, they found that the wetting properties of the Y<sub>2</sub>O<sub>3</sub>-Al<sub>2</sub>O<sub>3</sub>-SiO<sub>2</sub> eutectic melt controlled the densification behavior of the powder compact. The first stage was identified with the

formation of the ternary oxide eutectic and YAG. The shrinkage in this stage was due to the redistribution of liquid in the powder compact and slight improvement in the packing efficiency. The second stage was identified with the wetting of AlN particles and formation of  $\beta_{60}$ . The preferential wetting of AlN by the ternary oxide melt caused localization of the liquid, leading to a delaying effect on the second shrinkage step. The third stage occurred with the dissolution of  $\text{Si}_3\text{N}_4$  and formation of the final phase. Massive particle rearrangement was found to be the dominant densification mechanism. It also caused Al enrichment in the liquid, leading to formation of  $\beta_{60}$  as a transient phase. Thus the physical/chemical characteristics of the liquid, in particular its wetting behavior, and the kinetic pathway of the intermediate reactions are clearly important factors in reaction densification of multicomponent systems.

The preceding paper (part I)<sup>13</sup> has provided a broad picture of the wetting behavior of the ternary oxides and reaction pathways in the M-SiAlON system ( $M = \text{Li, Ca, Mg, Nd, Sm, Gd, Dy, Er, and Yb}$ ).<sup>13</sup> Generally, the more basic oxides wet  $\text{Si}_3\text{N}_4$ , whereas the more acidic oxides wet AlN. It has also identified temperatures for the various reactions which can be used to

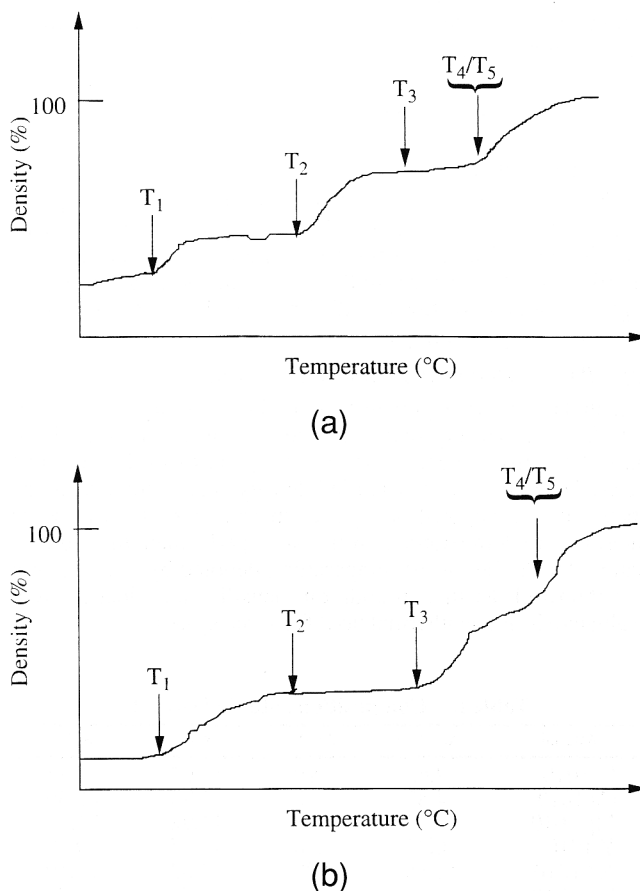


Fig. 1. Schematic shrinkage curves when the eutectic melt wets (a)  $\text{Si}_3\text{N}_4$ , and (b) AlN first.

S. C. Danforth—contributing editor

Manuscript No. 193383. Received August 3, 1994; approved October 17, 1994. Supported by the National Science Foundation under Grant No. DDM-9024975. \*Member, American Ceramic Society.

understand the shrinkage behavior. The reactions identified during the reaction densification of  $\alpha'$ -SiAlON are (i) the eutectic formation (at temperature  $T_1$ ), (ii) wetting of a nitride powder and intermediate phase precipitation (at temperature  $T_2$ ), (iii) secondary wetting of the other nitride powder (at temperature  $T_3$ ), (iv) dissolution of the intermediate phase (at temperature  $T_4$ ), and (v) precipitation of the final phase,  $\alpha'$ -SiAlON (at temperature  $T_5$ ).<sup>13</sup> Figures 1(a) and (b) show the schematic of expected shrinkage curves when the eutectic melt preferentially wets  $\text{Si}_3\text{N}_4$  and AlN, respectively. In these curves, the beginning of various shrinkage steps are identified with some of the above characteristic temperatures. Wetting of AlN is shown to lead to small or no immediate shrinkage in the powder compact because of the low AlN content of the typical SiAlON compact.<sup>12</sup> In Fig. 1(b), though, a subsequent shrinkage step occurs when the majority  $\text{Si}_3\text{N}_4$  is wetted. Variation of these shrinkage curves may also be possible. For example, it is known that the initial precipitation of the intermediate phase usually starts with partial wetting of the first nitride; i.e.,  $T_2$  could be significantly lower than the temperature when complete wetting is achieved.<sup>13</sup> Also, the dissolution of intermediate phase may or may not precede the precipitation of  $\alpha'$ -SiAlON;<sup>13</sup> i.e.,  $T_4$  may or may not be higher than  $T_5$ . Indeed  $T_4$  may even be lower than  $T_3$ , as shown later.

In this paper, we report the densification behavior during the reaction hot pressing of  $\alpha'$ -SiAlON system with metal oxide additions  $\text{M}_2\text{O}_3$ . Hot pressing was applied to provide a constant driving force for densification. The characteristic temperatures discussed above are identified for various systems using shrinkage data and information from part I. The role of wetting behavior of the ternary oxide melt and the formation/dissolution of intermediate phases in densification is then assessed along with other kinetic considerations such as amount and viscosity of the liquid. Some general conclusions are drawn from these comparisons to further our understanding of reaction densification of these complex systems.

## II. Experimental Procedure

### (1) Composition

The compositions investigated lie on the so-called  $\alpha'$ -plane represented by the formula  $\text{M}_p\text{Si}_{12-(m+n)}\text{Al}_{(m+n)}\text{O}_n\text{N}_{(16-n)}$ . Specifically,  $m = 1.0$ ,  $n = 1.0$  (1010), and  $m = 1.2$  and  $n = 1.0$  (1210) were chosen because they lie inside the single-phase  $\alpha'$  region. The compositions studied are listed in Table I and are the same as reported in part I.<sup>13</sup>

### (2) Powder Preparation and Hot Pressing

Details of powder preparation and hot pressing are given in part I.<sup>13</sup> Hot-pressing data reported here were obtained from runs at a constant heating rate of 15°C/min to 1750°C in most cases. The temperature when full density is obtained during the above runs is denoted as  $T_{100}$ . Isothermal runs held at some intermediate temperatures were also performed to approximately locate the lowest temperature, denoted by  $T_{\text{iso}}$ , required to obtain full density. In addition, densification kinetics were evaluated during isothermal hold for some systems.

Table I. Compositions Studied (wt%)

Material	Additive	$\text{Al}_2\text{O}_3$	AlN	$\text{Si}_3\text{N}_4$
Li 1010	2.63	2.99	12.03	82.35
Ca 1010	4.83	2.92	11.76	80.49
Mg 1010	3.52	2.96	11.92	81.60
Y 1010	6.37	2.88	11.57	79.18
Nd 1210	10.88	2.20	12.82	74.10
Sm 1210	11.24	2.19	12.76	73.81
Gd 1210	11.63	2.18	12.70	73.49
Dy 1210	11.93	2.17	12.66	73.24
Er 1210	12.20	2.16	12.62	73.02
Yb 1210	12.52	2.15	12.58	72.75

## III. Results

A summary of the densification behavior is given in Tables II and III. Table II gives the characteristic temperatures,  $T_1$ – $T_5$ , along with the volume shrinkage for the first two steps. Table III gives the two densification temperatures to reach full density,  $T_{100}$  and  $T_{\text{iso}}$ , as well as the phase assemblages at  $T_{\text{iso}}$ . The phase assemblages at  $T_{100}$  are already given in Table II of part I<sup>13</sup> for most of the systems.

### (1) Alkali and Alkaline-Earth Oxides

The systems studied here were M-1010, M being Li, Ca, and Mg.

(A) *Li System*: The shrinkage of the Li-1010 sample contains three well-defined stages (Fig. 2(a)). The first shrinkage step occurs at 1030°C accompanied by 5% shrinkage. The second step occurs at 1225°C, accompanied by 20% shrinkage. The third step occurs at 1500°C. A fourth step occurs at 1600°C. Full density is achieved at 1750°C under constant heating rate and can also be achieved at 1550°C when held over 20 min.

For this system, in which wetting of  $\text{Si}_3\text{N}_4$  is preferred and is complete at 1350°C,<sup>13</sup> the characteristic temperatures are  $T_1 = 1010^\circ\text{C}$  and  $T_2 = 1210^\circ\text{C}$ , corresponding to the formation of oxide melt, and the wetting of  $\text{Si}_3\text{N}_4$ , respectively. The third shrinkage step starting at 1500°C seems to correspond to the dissolution of the intermediate phase O' (1550°C, hence at  $T_4$ ). Since  $\alpha'$  formation was detected above 1420°C ( $T_5$ ), according to part I,<sup>13</sup> yet AlN still remained at 1550°C after isothermal hold but not at 1750°C,<sup>13</sup> the step at 1600°C is possibly related to wetting and dissolution of AlN ( $T_3$ ).

(B) *Ca System*: Compared to Li-1010, the shrinkage curve of Ca-1010 has fewer well-separated steps (Fig. 2(b)). However, on closer examination, three shrinkage steps can be identified. The first shrinkage step occurs at 1360°C. A second step is identified around 1410°C, followed by continuous gradual shrinkage. A third step at 1610°C and another at 1660°C seem to be present. Full density can be achieved at 1750°C under constant heating rate and also at 1650°C when held for 25 min. Full densification was not possible at 1550°C.

For this system, in which  $\text{Si}_3\text{N}_4$  is preferentially and completely wetted at 1450°C, we can identify  $T_1 = 1360^\circ\text{C}$  and  $T_2 = 1410^\circ\text{C}$ . They correspond to the formation of eutectic and wetting of  $\text{Si}_3\text{N}_4$ , respectively, like the Li system. The third shrinkage step again appears to be due to the dissolution of O' ( $T_4$ ). Lastly, since some  $\alpha'$  already has formed at 1550°C ( $T_5$ ) and AlN remains at 1650°C after isothermal hold,<sup>13</sup> the step at 1660°C is possibly due to AlN wetting and dissolution ( $T_3$ ).

(C) *Mg System*: Mg-1010 was found to be very difficult to densify. Under constant heating conditions only 83% dense samples were obtained at 1850°C. Distinct shrinkage steps can easily be identified (Fig. 2(c)). One distinct step occurs at 1525°C, although a smaller step at 1350°C seems also discernible. Another distinct step was found at 1630°C. Although a number of additional shrinkage steps, whose positions were found to vary from run to run, exist between 1630° and 1850°C, densification is sluggish. The origin of this sluggish densification is the formation of a highly refractory  $\text{Mg}_2\text{Al}_4\text{Si}_5\text{O}_{18}$  following wetting of  $\text{Si}_3\text{N}_4$ .<sup>13</sup> This compound does not melt even at 1850°C and it deprives the compact of the sintering liquid.

The characteristic temperatures identified for this system are as follows:  $T_1 = 1350^\circ\text{C}$  corresponding to formation of eutectic and  $T_2 = 1525^\circ\text{C}$  corresponding to  $\text{Si}_3\text{N}_4$  wetting and formation of  $\text{Mg}_2\text{Al}_4\text{Si}_5\text{O}_{18}$ . In addition, the step at 1630°C is very likely due to AlN wetting, hence  $T_3 = 1630^\circ\text{C}$ . The steps at higher temperatures vary in position, probably because of the heterogeneous nature of the very slow reaction of AlN in the presence of the small amount of liquid. The dissolution temperature of the intermediate phase is very high ( $T_4 > 1850^\circ\text{C}$ ) while the formation temperature of  $\alpha'$  is 1570°C ( $T_5$ ).

### (2) Rare Earths

The shrinkage curves of these materials are shown in Figs. 3–6, all hot pressed to 1750°C. Under constant heating

**Table II. Summary of Features of the Shrinkage Curves for Samples Hot Pressed at a Heating Rate of 15°C/min**

System	$T_1$ (°C)	$T_2$ (°C)	$T_3$ (°C)	$T_4$ (°C)	$T_5$ (°C)	Volume shrinkage (%)	
						First stage	Second stage
Li	1010	1225	1600	1500	1420	8.0	15.0
Ca	1360	1450	1660	1610	1550	5.0	28.0
Mg	1350	1500	1630	>1850	1575	5.0	9.0
Nd	1400	1450	1580	~1800	1420	4.0	15.0
Sm	1380	1460	1600	~1800	1420	7.0	17.0
Gd	1370	1500	1620	1700	1575	7.0	10.0
Dy	1360	~1500	1560		1575/1675	5.0	20
Er	1400	~1500	1580	1640	1580	4.0	13.0
Yb	1380	~1500	1560	1640	1560	9.0	10.0

**Table III. Lowest Temperature to Reach Full Density under Constant Heating Rate ( $T_{1000}$ ) or under Isothermal Hold ( $T_{iso}$ )**

System	$T_{100}$ at 15°C/min	$T_{iso}$ , time	Phase assemblage at $T_{iso}$
Li	1750°C	1550°C, 20 min	$\alpha'$ , O', AlN
Ca	1750°C	1650°C, 25 min	$\alpha'$ , O', AlN
Mg	>1850°C	>1850°C	$\alpha'$ , $\mu$ -cordierite,* AlN
Nd	1720°C	1720°C, 0 min	$\alpha'$ , M', AlN
Sm	1750°C	1750°C, 0 min	$\alpha'$ , M', AlN
Gd	1750°C	1675°C, 30 min	M', $\alpha'$ , AlN
Dy	>1750°C	1575°C, 35 min	$\alpha'$
Er	1740°C	1575°C, 37 min	$\alpha'$ , $\beta'$
Yb	1750°C	1575°C, 40 min	$\alpha'$ , $\beta'$

\*Mg<sub>2</sub>Al<sub>4</sub>Si<sub>2</sub>O<sub>18</sub>

rate, densification was reached at 1750°C for four systems, Nd, Sm, Gd and Yb, whereas Dy-1210 and Er-1210 required additional holding time at 1750°C to reach full density.

Interestingly, when held at 1570°C for about 40 min, the heavier rare earths, Dy-, Er-, Yb-containing systems, did reach full density, but not the lighter rare earths, Nd-, Sm-, and Gd-containing systems. When hot pressed at 1675°C with a hold time of 30 min, Gd- and Dy-containing systems reached full density, whereas Nd- and Sm-containing systems did not. Thus, very different hot-pressing behavior is evident for these samples. In the following, we divide these rare earths into three groups describing our observations separately.

(A) *Lighter Rare Earths (Nd, Sm)*: Shrinkage curves of these samples are somewhat similar (Figs. 3(a) and (b)). The first shrinkage step occurs at 1400°C for Nd and 1360°C for Sm, followed by a second shrinkage step at 1450–1460°C. A third shrinkage step is found above 1550°C. However, since this shrinkage step appears to accelerate again at higher temperatures, the third stage cannot be clearly identified and may occur at higher temperature for Sm than for Nd.

For this system in which Si<sub>3</sub>N<sub>4</sub> is preferentially wetted (complete at 1550°C), we identify  $T_1 = 1400^\circ\text{C}$  and  $1360^\circ\text{C}$  for eutectic melting, and  $T_2 = 1450^\circ\text{C}$  and  $1460^\circ\text{C}$  for Si<sub>3</sub>N<sub>4</sub> wetting, for Nd and Sm systems, respectively. For melilite dissolution,  $T_4$  is probably around  $1800^\circ\text{C}$ .<sup>13</sup> For  $\alpha'$  formation,  $T_5$  is as low as  $1420^\circ\text{C}$  according to I.<sup>13</sup> The third shrinkage step is probably due to the dissolution of AlN in the melt, which according to the wetting experiments, should occur at  $1600^\circ\text{C}$  ( $T_3$ ). As mentioned before, these samples densify easily at  $1750^\circ\text{C}$  but not at  $1575^\circ\text{C}$  or  $1675^\circ\text{C}$ . In both cases, the intermediate phase, M', is retained. Some unreacted AlN also tends to remain up to  $1750^\circ\text{C}$ .

(B) *Heavier Rare Earths (Er, Yb)*: Shrinkage curves of these samples (Figs. 4(a) and (b)) contain a shrinkage step around  $1400^\circ\text{C}$ . The shrinkage in the Yb-containing sample at this step is more than that in Er-1210. The next shrinkage step occurs at around  $1580^\circ\text{C}$  and the third step occurs at around  $1640^\circ\text{C}$ . As mentioned before, Yb-1210 reaches full density at  $1750^\circ\text{C}$  in the schedule of constant heating rate. However, Er-1210 densifies somewhat slower and requires somewhat higher temperature. Unlike lighter rare-earth samples, both can reach

full density at  $1575^\circ\text{C}$ . The above behavior is similar to that of Y-containing materials reported by Hwang and Chen.<sup>12</sup>

For this system in which AlN is preferentially wetted (complete at  $1550^\circ\text{C}$ ), we identify  $T_1 = 1400^\circ\text{C}$ , for eutectic formation, and  $T_3 = 1580^\circ\text{C}$ , for Si<sub>3</sub>N<sub>4</sub> wetting for both the Er and Yb systems. Wetting of AlN is probably at a lower temperature ( $T_2 = 1500^\circ\text{C}$ ), since the intermediate phase,  $\beta_{60}$ , is already formed at  $1575^\circ\text{C}$  (see Table III in part I) and AlN has disappeared. However, it does not result in a distinct shrinkage step (Figs. 4(a) and (b)). Instead, the slow shrinkage duration following  $T_1$  is much longer in Er and Yb systems compared to Nd and Sm systems. This is probably a manifestation of the delaying effect of AlN wetting, which tends to localize the oxide melt according to a previous study of Hwang and Chen.<sup>12</sup> Lastly,  $\beta'$ -SiAlON disappears before  $1750^\circ\text{C}$  when only  $\alpha'$  remains.<sup>13</sup> Thus, the third shrinkage step at around  $1650^\circ\text{C}$  could be associated with  $T_4$ . The formation of  $\alpha'$  begins at  $1575^\circ\text{C}$  ( $T_5$ ) according to part I.<sup>13</sup>

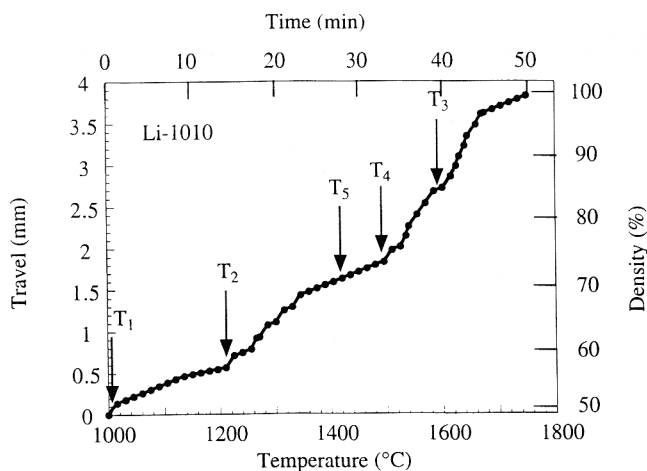
(C) *Intermediate Rare Earths (Gd, Dy)*: The two intermediate rare earth systems, Gd-1210 and Dy-1210, have more complicated shrinkage curves. They can be compared with those of lighter and heavier rare-earth systems which clarify the behavior. These are described below.

Essentially Gd-1210 is found to behave similarly to the lighter rare earths, Nd and Sm systems, with a  $T_1 = 1370^\circ\text{C}$ ,  $T_2 = 1500^\circ\text{C}$ , and  $T_3 = 1620^\circ\text{C}$  shown in Fig. 5(a). As reported in part I,<sup>13</sup> melilite formed in Gd-1210 at intermediate temperature disappeared before  $1750^\circ\text{C}$ . This gives rise to an additional shrinkage step at around  $1700^\circ\text{C}$  ( $T_4$ ) and possibly some fine feature at  $1660^\circ\text{C}$  in the shrinkage curve shown in the Fig. 6(a). In addition, the dissolution of melilite makes it possible to densify Gd-1210 at  $1675^\circ\text{C}$  to full density, when held for 30 min. Densification at  $1750^\circ\text{C}$  is also achieved under constant heating rate, as in the case for Nd-1210 and Sm-1210, but without melilite remaining. Formation temperature of  $\alpha'$  is again at  $1575^\circ\text{C}$  ( $T_5$ ) according to part I.<sup>13</sup>

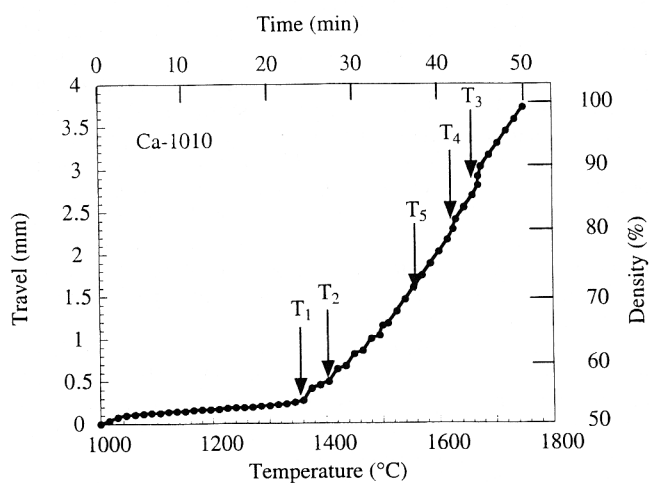
Dy-1210 is found to behave similarly to the heavier rare earths, Er-1210 and Yb-1210. In this case,  $T_1 = 1360^\circ\text{C}$  and  $T_3 = 1560^\circ\text{C}$  as shown in Fig. 5(b). A long delay above  $T_1$  is also seen, presumably due to AlN trapping the liquid. Phase analysis in part I, however, found that the  $\alpha'$  formed at  $1575^\circ\text{C}$  has an unusually strong (200) reflection and that the intermediate  $\beta'$  does not exist at  $1575^\circ\text{C}$ .<sup>13</sup> Also the densification rate in the last stage (above  $1650^\circ\text{C}$ ) is very slow. These unusual features are partly due to the high viscosity of Dy containing Si-Al-O-N melt in the system.<sup>14,15</sup> In addition we found from lattice parameters measured of annealed specimens that the lattice suddenly expands at  $1675^\circ\text{C}$  (see Fig. 6). This strongly suggests a shift of solubility limit, expanding the single  $\alpha'$ -phase region, at above  $1650^\circ\text{C}$ . It can cause further precipitation of  $\alpha'$  ( $T_5' = 1675^\circ\text{C}$ ) and depletion of Dy from the melt. This reaction renders the liquid even more viscous, making Dy-1210 the hardest rare-earth SiAlON to densify at  $1750^\circ\text{C}$ .

### (3) Kinetics of Isothermal Shrinkage

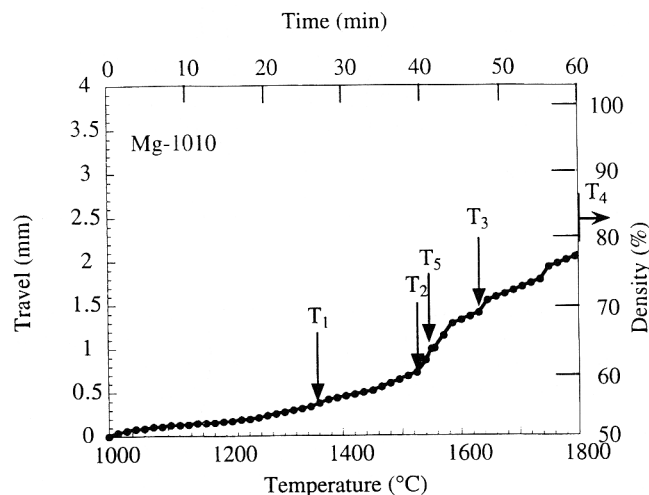
Data of isothermal shrinkage as a function of hold time are plotted in Fig. 7 for the following systems: Ca-1010 at  $1550^\circ\text{C}$ ,



(a)

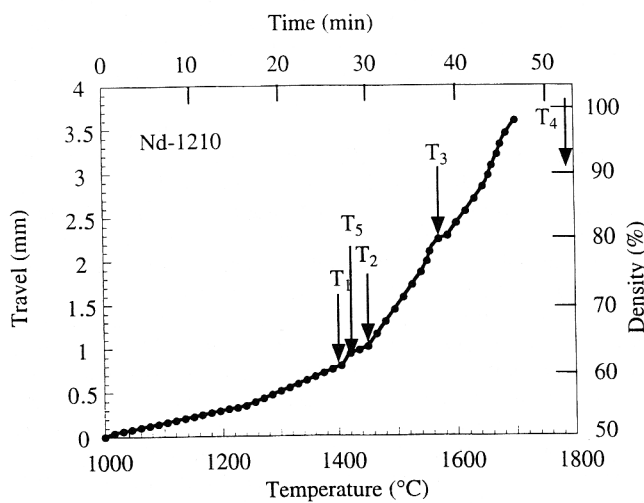


(b)

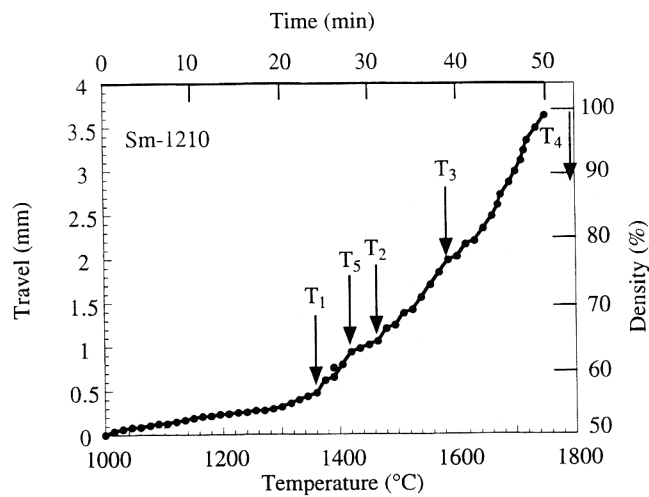


(c)

Fig. 2. Shrinkage curve for (a) Li-1010, (b) Ca-1010, and (c) Mg-1010 hot pressed at a constant heating rate of 15°C/min, showing the characteristic temperatures.



(a)



(b)

Fig. 3. Shrinkage curve for (a) Nd-1210 and (b) Sm-1210, hot pressed at a constant heating rate of 15°C/min, showing the characteristic temperatures.

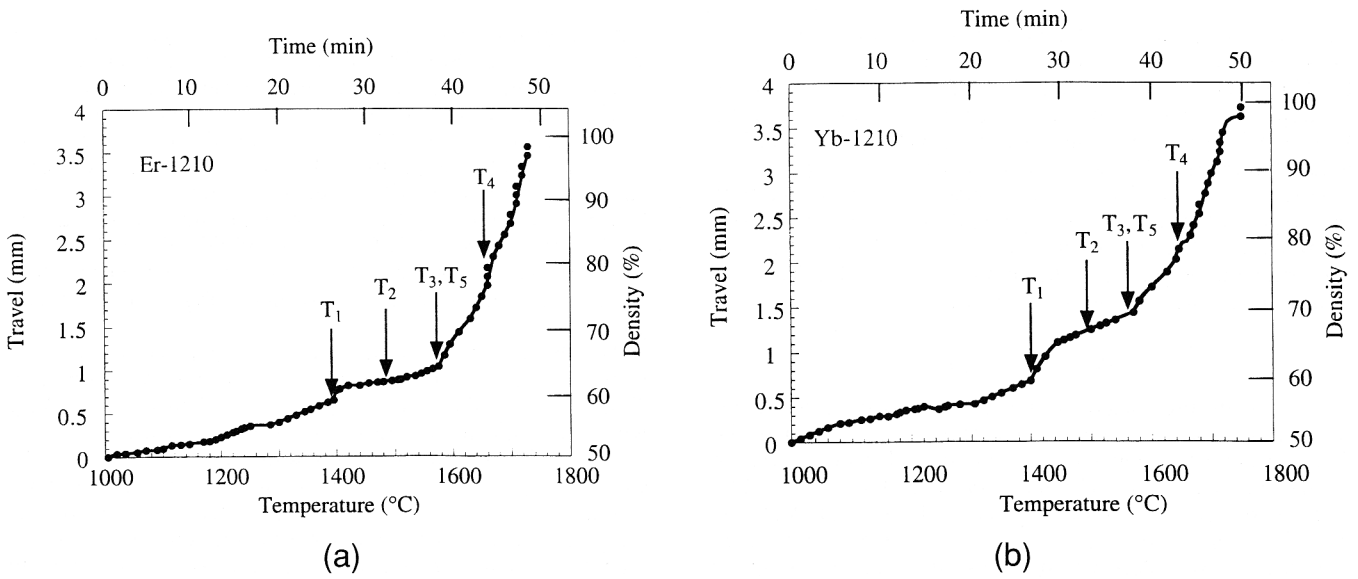


Fig. 4. Shrinkage curve for (a) Er-1210 and (b) Yb-1210, hot pressed at a constant heating rate of 15°C/min, showing the characteristic temperatures.

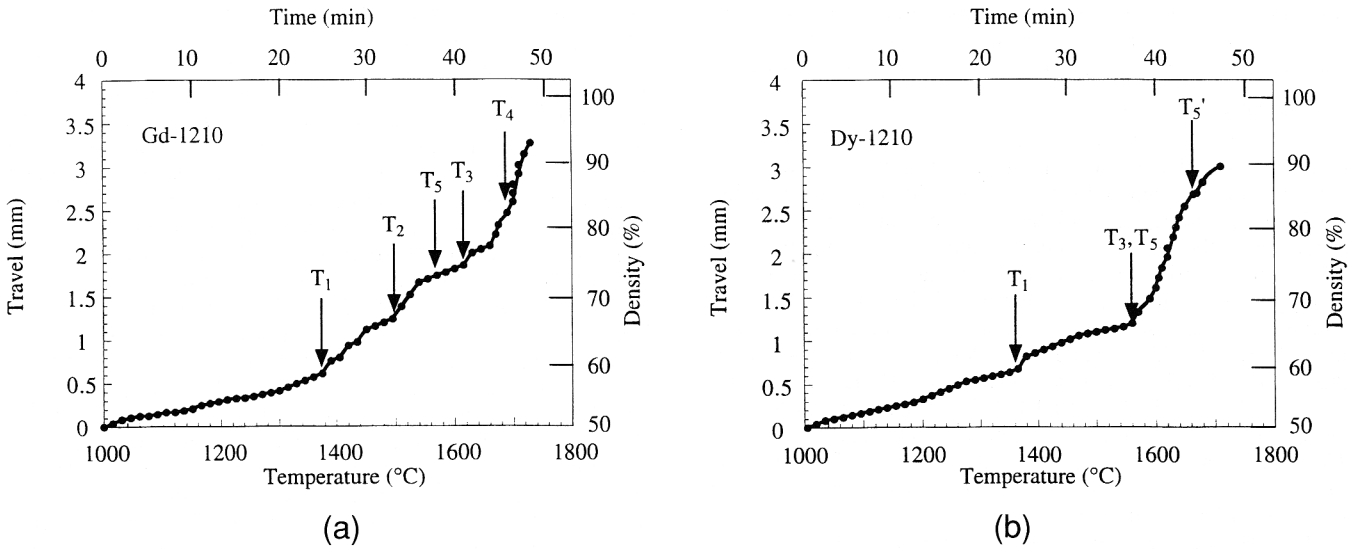


Fig. 5. Shrinkage curve for (a) Gd-1210 and (b) Dy-1210, hot pressed at a constant heating rate of 15°C/min, showing the characteristic temperatures.

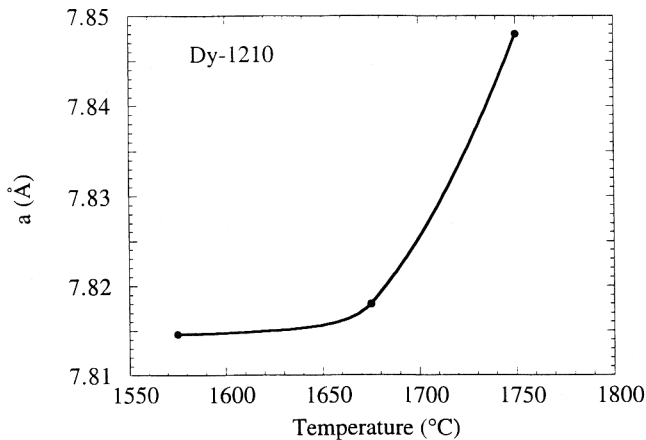


Fig. 6. Lattice parameter  $a$ , for Dy- $\alpha'$ -SiAlON as a function of temperature.

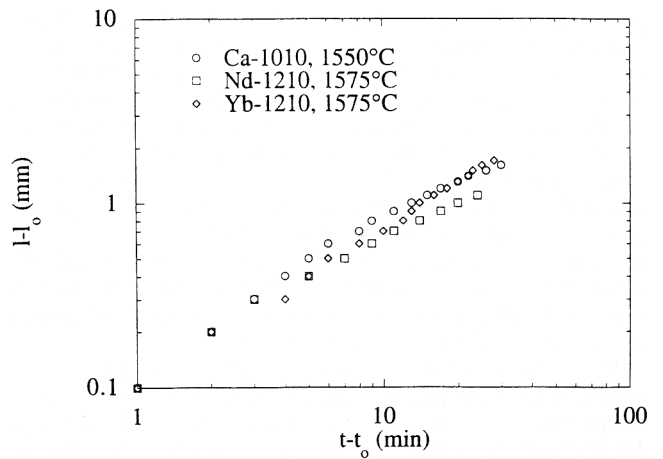


Fig. 7. Isothermal shrinkage in  $\log(L_0 - L)$  vs  $\log(t_0 - t)$  for Ca-1010 at 1550°C, Nd-1210, and Yb-1210 at 1575°C.

and Nd-1210 and Yb-1210, both at 1575°C. At these temperatures, isothermal hold brought the density to ~90% for Ca-1010, 80% for Nd-1210, and 100% for Yb-1210. The slopes of these plots, in logarithm scale, serve as an indicator of the likely mechanism of densification. Based on Kingery's model,<sup>16</sup> a dissolution/precipitation process gives rise to a slope of 1/3, whereas a higher slope is attributed to massive particle rearrangement in the presence of liquid. In all cases examined, we found the slope invariably greater than 0.5. Thus, dissolution/precipitation cannot be the dominant process for densification in these materials until very high density.

#### IV. Discussion

The densification behavior of Si-Al-M-O-N systems is complicated because of the involvement of two nitride powders, the formation of intermediate phases, and the substantial variation of melt viscosity and acidity/basicity depending on the  $M_2O_3$  additive present. In a previous study,<sup>9</sup> the role of AlN was investigated in the Si-Al-Y-O-N system in which the oxide melt preferentially wets AlN. Our previous study further examines a number of other systems encompassing preferential wetting of either AlN or  $Si_3N_4$ .<sup>13</sup>

Although the detailed densification behavior and reaction and reaction sequences vary, some general trends can be discerned from a comparison of characteristic temperatures. Along with our qualitative knowledge of the viscosity of these systems, a clear picture now emerges as depicted in the following.

##### (1) Characteristic Temperatures

(A) *Formation of Ternary Eutectic Oxide Melt ( $T_1$ ):* The first major shrinkage step is associated with this reaction. The densification mechanism in this stage is primarily redistribution of liquid, resulting in a slight improvement in the packing efficiency of the powder compact. Although the temperature of this reaction varies, it rarely provides any indication of the subsequent densification behavior. This is because of the small amount of oxide liquid formed, estimated to be around 5 vol% in most cases.<sup>17-19</sup> The resultant shrinkage is relatively small, of the order of 5 vol%, as evident from Table II. Thus, despite a very low  $T_1$  of 1010°C in Li-1010, full density is not reached until 1750°C ( $T_{100}$ ), in a constant heating rate schedule or until 1550°C ( $T_{iso}$ ) with an isothermal hold. In contrast,  $T_{100}$  is 1720°C in Nd-1210 and  $T_{iso}$  is 1575°C for Er-1210, despite a much higher  $T_1$  of 1400°C in both.

(B) *Wetting of Nitride Powders and Formation of Intermediate Phases ( $T_2$  and  $T_3$ ):* The second major shrinkage step is associated with the wetting of the majority nitride,  $Si_3N_4$ . If AlN, the minority nitride, is wetted preferentially, no shrinkage step is observed at  $T_2$  and the duration of slow shrinkage after  $T_1$  is prolonged until  $T_3$  as shown in Fig. 1(b). This was previously observed in Y-SiAlON<sup>9</sup> and is now further verified in heavier rare-earth SiAlONs ( $M = Dy, Er, \text{ and } Yb$ ). In these cases, liquid is thought to be trapped at AlN particles and not spread out, so that the powder compact is effectively "dry." On the other hand, if  $Si_3N_4$  is wetted preferentially, then a gradual but substantial shrinkage step at  $T_2$  is always seen, resulting in shrinkage of the order of 10% or more. In addition, another shrinkage step at  $T_3$  corresponding to AlN wetting can also be seen, also leading to substantial shrinkage over time. This is evident in systems where  $M = Li, Ca, Mg, Nd, Sm, \text{ and } Gd$ . Thus the second shrinkage step at either  $T_2$  (if  $Si_3N_4$  wetted first) or  $T_3$  (if AlN wetted first), is always associated with the wetting of majority nitride powder. From Table II, it can be seen that the shrinkage at this step is of the order of 10% or more.

(C) *Dissolution Melting of Intermediate Phase ( $T_4$ ):* Dissolution/melting of intermediate phase, when it occurs at lower temperatures, usually results in a shrinkage step. This is seen in Li-1010 and Ca-1010 for O'-SiAlON dissolution, Gd-1210 for M' melting, and Er-1210 and Yb-1210 for  $\beta'$ -SiAlON dissolution. (However, we did not see a distinct shrinkage step ascribed to  $\beta'$ -SiAlON dissolution in Dy-1210, presumably because of

very sluggish kinetics in this highly viscous system that limit the amount of  $\beta'$ -SiAlON formed upon  $T_4$ ). In other systems, where  $T_4$  is higher, hot pressing under constant heating rate can reach full density slightly below  $T_4$ . This is the case of Nd-1210 and Sm-1210, for which M' melts at around 1800°C<sup>20</sup> but  $T_{100}$  is 1720° and 1730°C, respectively. In both cases, the dense bodies obtained still contain M', as shown in Table II of part I.<sup>13</sup> However, if the melting/dissolution temperature is too high, as in Mg-1010 for  $Mg_2Al_4Si_5O_{18}$  ( $T_4 > 1850^\circ\text{C}$ ), then full density cannot be reached even at 1850°C. Thus, the final densification is often associated with dissolution/melting of intermediate phase.

The above comparison suggests that  $T_4$  can place an approximate lower limit for full densification temperature. Referring to Table III, we find  $T_{iso}$  to lie approximately between  $T_3$  and  $T_4$ , when the temperatures are relatively close to each other, e.g., within 100°C of each other. This is the case with  $M = Li, Ca, Gd, Dy, Er, \text{ and } Yb$ . In all of the above systems, the phase assemblage at  $T_{iso}$  and full density still contains some intermediate phases. This implies that some dissolution and melting of intermediate phase are necessary for full densification, although full reaction is not required if isothermal hold is applied. On the other hand, when  $T_4$  is much higher than  $T_3$ , then either  $T_{iso} \approx T_{100}$  and no distinct third step is seen, as in Nd-1210 and Sm-1210 of full densification is difficult anyway, as in Mg-1010. On the other hand, when  $T_3$  and  $T_4$  are close to each other, then  $T_{iso}$  is much less than  $T_{100}$ .

It is clear that in order to achieve full densification at relatively low temperature, relatively low temperature for wetting of second nitride ( $T_3$ ) and dissolution/melting of the intermediate phase ( $T_4$ ) are required. The latter is required primarily to resupply the liquid necessary for densification. In the special case when very little intermediate phase is precipitated and hence very little liquid is expended,  $T_4$  is irrelevant and full density can be reached essentially at  $T_3$ . This is illustrated in the case of Dy-1210 where  $T_{iso}$  is nearly 200°C lower than  $T_{100}$ .

(D) *Formation of  $\alpha'$ -SiAlON ( $T_5$ ):* In most cases studied here,  $T_5$  is found to be at relatively low temperature so that it is of little consequence in determining the densification temperature. The only exception is seen in Dy-1210, where formation of  $\alpha'$ -SiAlON apparently occurs in two stages, first at above 1500°C but with low solute concentration, then above 1675°C and with a much higher solute concentration. The secondary  $\alpha'$  precipitation has an important effect of arresting shrinkage, so that only 90% density is reached even at 1750°C when a constant heating rate is used. As mentioned before, this observation can be understood by the effect of secondary  $\alpha'$  formation on the amount of the liquid, and possibly its viscosity as well. This material must be densified by holding at below  $T_5'$ .

The characteristic temperatures, except  $T_1$ , are expected to vary with the composition. In fact,  $T_1$  is expected to be independent of composition in systems with one eutectic in the  $M_2O_3$ - $Al_2O_3$ - $SiO_2$  system at low nitrogen content. In systems like Ca or Mg with more than one eutectic in the  $M_2O_3$ - $Al_2O_3$ - $SiO_2$  system,  $T_1$  will depend on the initial oxide composition. The values of  $T_2$ ,  $T_3$  and  $T_4$  are dictated by the basicity of the melt which controls the wetting behavior and hence the formation of the intermediate phases.<sup>13</sup> For example, moving toward the  $Al_2O_3$  corner on the  $\alpha'$ -SiAlON will decrease the basicity of the melt, resulting in an increase in the value of  $T_2$  and a decrease in the value of  $T_3$ . The value of  $T_4$  will depend on the intermediate phase formed. For example, decreasing the amount of  $Al_2O_3$  is expected to result in formation of intermediate phases with a higher Si/Al ratio, which will change the value of  $T_4$ . The value of  $T_5$  is also expected to change with composition. Higher basicity is expected to result in a decrease in the value of  $T_5$ .

##### (2) Amount and Viscosity of Liquid

Liquid phase is obviously of central importance for densification of M-SiAlON. The amount of the liquid in the first stage upon eutectic melt formation is determined by the phase diagram.<sup>17-19</sup> The amount of liquid in the tertiary stage is



affected by the dissolution/melting of the intermediate phase, and in special cases even by the secondary precipitation of  $\alpha'$ -SiAlON. In addition, the distribution of liquid is also relevant, as in the case of the preferential wetting of AlN. In all circumstances, when the amount of liquid is severely reduced because of precipitation or localization, densification is retarded.

Viscosity of the liquid is also expected to have an effect on the densification kinetics. This effect, however, is obscured in most cases by the different characteristic temperatures that vary widely among various systems. For example, although the density achieved under constant heating rate decreases in the order of Nd, Sm, and Gd, reflecting the increasing viscosity in the same order,<sup>14,15</sup> at above 1700°C this trend is countered by the decreasing melting temperature of  $M'$  ( $T_4$ ) in the same order, resulting in very rapid densification of Gd-1210. (The faster kinetics of Gd-1210 at 1750°C are also confirmed by the lattice parameter data of  $\alpha'$ -SiAlON in Table I of part I,<sup>10</sup> where the cell size of Gd  $\alpha'$ -SiAlON at 1750°C is seen to be much larger than that of Nd-1210 and Sm-1210, even though the Gd ion is smaller.)

Likewise, in heavier rare-earth SiAlONs, although we found in isothermal hot pressing that the densification time at 1575°C increases slightly in the order of Dy, Er, and Yb, probably due to the influence of viscosity, the densification kinetics in constant heating rate do not reflect the same trend, because of nonmonotonic variation of characteristic temperatures.

## V. Conclusions

(1) Reaction densification of M-SiAlON occurs in three stages. The first stage is associated with the formation of the  $\text{SiO}_2\text{-Al}_2\text{O}_3\text{-M}_2\text{O}_3$  ternary eutectic (at temperature  $T_1$ ). The second stage is associated with the preferential wetting of majority nitride powder  $\text{Si}_3\text{N}_4$ . This occurs at  $T_2$  when  $\text{Si}_3\text{N}_4$  is wetted first. If AlN is wetted first, then no shrinkage step is observed at  $T_2$  and the densification is delayed until  $T_3$ , when  $\text{Si}_3\text{N}_4$  is wetted finally.

(2) The third stage involves the dissolution/melting of the intermediate phase (at temperature  $T_4$ ) if  $T_4$  is low; otherwise a distinct third stage is not seen while a gradual densification continues following the second stage. In the extreme case of very high  $T_4$ , this may result in poor density as in the case of Mg-1010.

(3) The formation temperature ( $T_5$ ) of the final  $\alpha'$ -SiAlON phase is not crucial in most cases, unless a sudden secondary precipitation of  $\alpha'$ -SiAlON at the later stage ( $T_5'$ ) drains the liquid and retards densification. Such material must be densified at temperatures below  $T_5'$ .

(4) To achieve full densification at relatively low temperature, a low wetting temperature for the second nitride ( $T_3$ ) and low dissolution/melting temperature of the intermediate phase ( $T_4$ ) are required.

(5) The dominant process for densification in these materials is massive particle rearrangement, although some dissolution facilitates full densification by providing the necessary

liquid. More generally, the amount of liquid is controlled by the phase diagram, dissolution/melting of intermediate phase, distribution of liquid, and secondary precipitation of  $\alpha'$ -SiAlON.

(6) The effect of viscosity of liquid is relatively insignificant compared to that of the amount of liquid for reaction densification of  $\alpha'$ -SiAlON.

## References

- <sup>1</sup>P. Drew and M. H. Lewis, "The Microstructure of Silicon Nitride Ceramics during Hot-Pressing Transformations," *J. Mater. Sci.*, **9**, 261-69 (1974).
- <sup>2</sup>M. H. Lewis, B. D. Powell, P. Drew, R. J. Lumby, B. North, and A. J. Taylor, "The Formation of Single-Phase Si-Al-O-N Ceramics," *J. Mater. Sci.*, **12**, 61-74 (1977).
- <sup>3</sup>M. H. Lewis, A. R. Bhatti, R. J. Lumby, and B. North, "The Microstructure of Sintered Si-Al-O-N Ceramics," *J. Mater. Sci.*, **15**, 103-13 (1980).
- <sup>4</sup>M. H. Lewis and R. J. Lumby, "Nitrogen Ceramics: Liquid Phase Sintering," *Powder Metall.*, **26** [2] 73-81 (1983).
- <sup>5</sup>G. K. Layden, "Process Development for Pressureless Sintering of SiAlON Ceramic Components," Report No. R175-91072-4. United Technologies Research Center, Feb. 1976.
- <sup>6</sup>S. Boskovic, L. J. Gauckler, G. Petzow, and T. Y. Tien, "Reaction Sintering Forming  $\beta$ - $\text{Si}_3\text{N}_4$  Solid Solution in the System Si,Al/N,O I: Sintering of  $\text{Si}_3\text{N}_4$ -AlN Mixtures," *Powder Metall. Int.*, **9** [4] 185-89 (1977).
- <sup>7</sup>S. Boskovic, L. J. Gauckler, G. Petzow, and T. Y. Tien, "Reaction Sintering Forming  $\beta$ - $\text{Si}_3\text{N}_4$  Solid Solution in the System Si,Al/N,O II: Sintering of  $\text{Si}_3\text{N}_4$ - $\text{SiO}_2$ -AlN Mixtures," *Powder Metall. Int.*, **10** [4] 180-85 (1978).
- <sup>8</sup>S. Boskovic, L. J. Gauckler, G. Petzow, and T. Y. Tien, "Reaction Sintering Forming  $\beta$ - $\text{Si}_3\text{N}_4$  Solid Solution in the System Si,Al/N,O III: Sintering of  $\text{Si}_3\text{N}_4$ -AlN- $\text{Al}_2\text{O}_3$  Mixtures," *Powder Metall. Int.*, **11** [4] 169-71 (1979).
- <sup>9</sup>M. N. Rahman, F. L. Riley, and R. J. Brook, "Mechanisms of Densification during Reaction Hot-Pressing in the System Si-Al-O-N," *J. Am. Ceram. Soc.*, **63** [11-12] 648-53 (1980).
- <sup>10</sup>M. Kubawara, M. Benn, and F. L. Riley, "The Reaction Hot Pressing of Compositions in the System Al-Si-O-N Corresponding to  $\beta'$ -SiAlON," *J. Mater. Sci.*, **15**, 1407-16 (1980).
- <sup>11</sup>M. Havner and P. L. Hansen, "Hot-Pressing and  $\alpha$ - $\beta'$  Phase Transformation of Compositions Corresponding to  $\beta'$ -SiAlON," *J. Mater. Sci.*, **25**, 992-96 (1990).
- <sup>12</sup>S. L. Hwang and I-Wei Chen, "Reaction Hot Pressing of  $\alpha'$ - and  $\beta'$ -SiAlON Ceramics," *J. Am. Ceram. Soc.*, **77** [1] 165-71 (1994).
- <sup>13</sup>M. Menon, and I-Wei Chen, "Reaction Densification of  $\alpha'$ -SiAlON: I, Wetting Behavior and Acid-Base Reactions," *J. Am. Ceram. Soc.*, **78** [3] 545-52 (1995).
- <sup>14</sup>J. E. Shelby and J. T. Kohli, "Rare-Earth Aluminosilicate Glasses," *J. Am. Ceram. Soc.*, **73** [1] 39-42 (1990).
- <sup>15</sup>K. P. J. O'Reilly, M. Redington, S. Hampshire, and M. Liegh, "Parameters Affecting Pressureless Sintering of  $\alpha'$ -SiAlONs with Lanthanide Modifying Cations"; pp. 393-98 in *Silicon Nitride Ceramics Scientific and Technological Advances*, Proceedings of Materials Research Society Symposium, 287 (Boston, MA, Nov. 30-Dec. 3, 1992). Edited by I-Wei Chen, P. F. Becher, M. Mitomo, G. Petzow, and T. S. Yen. Materials Research Society, Pittsburgh, PA, 1993.
- <sup>16</sup>W. D. Kingery, J. M. Woulbroun, and F. R. Charvat, "Effects of Applied Pressure on Densification during Sintering in Presence of a Liquid Phase," *J. Am. Ceram. Soc.*, **46** [8] 391-95 (1963).
- <sup>17</sup>E. M. Lewis, C. R. Robbins, and H. F. McMurdie, Figs. 459 for Li, 630 for Ca, 712 for Mg, and 2586 for Y in *Phase Diagrams for Ceramists*. Edited by M. K. Reser. American Ceramic Society, Columbus, OH, 1969.
- <sup>18</sup>E. M. Erbe, and D. E. Day, "Properties of  $\text{Sm}_2\text{O}_3\text{-Al}_2\text{O}_3\text{-SiO}_2$  Glasses for in Vivo Applications," *J. Am. Ceram. Soc.*, **73** [9] 2708-13 (1990).
- <sup>19</sup>Y. Murakami and H. Yamamoto, "Phase Equilibria and Properties of Glasses in the  $\text{Al}_2\text{O}_3\text{-Yb}_2\text{O}_3\text{-SiO}_2$  System," *J. Ceram. Soc. Jpn.*, **101** [10] 1101-106 (1993).
- <sup>20</sup>Y. B. Cheng and D. P. Thompson, "Aluminum-Containing Nitrogen Melilite Phases," *J. Am. Ceram. Soc.*, **77** [1] 143-48 (1994). □